

## Electronic Supplementary Information (ESI)

### **Rational structural design of benzothiazolium-based crystal HDB-T with high nonlinearity and efficient terahertz-wave generation**

**Jingkai Shi,<sup>a</sup> Fei Liang,<sup>b</sup> Yixin He,<sup>c</sup> Xinyuan Zhang,<sup>\*a</sup> Zheshuai Lin,<sup>b</sup> Degang  
Xu,<sup>c</sup> Zhanggui Hu,<sup>a</sup> Jianquan Yao,<sup>c</sup> and Yicheng Wu<sup>a</sup>**

*<sup>a</sup>Tianjin Key Laboratory of Functional Crystal Materials, Institute of Functional  
Crystals, Tianjin University of Technology, Tianjin 300384, PR. China. Email:  
xyzhang@email.tjut.edu.cn*

*<sup>b</sup>Beijing Center for Crystal Research and Development, Key Laboratory of Functional  
Crystals and Laser Technology, Technical Institute of Physics and Chemistry,  
Chinese Academy of Sciences, Beijing 100190, PR. China.*

*<sup>c</sup>The Institute of Laser & Optoelectronics, College of Precision Instruments and Opto-  
electronics Engineering, Tianjin University, Tianjin 300072, China.*

## 1. Experimental

### Synthesis

*Synthesis of 2-(4-hydroxy-3,5-dimethylstyryl)-3-methylbenzo[d]thiazol-3-ium 4-methylbenzenesulfonate (HDB-T):* 2-Methylbenzothiazole (29.84 g, 0.2 mol) and methyl 4-methylbenzenesulfonate (37.25 g, 0.2 mol) were dissolved in 1,2-dimethoxyethane (250 mL). The solution was stirred at 60 °C for 48 h and then cooled to room temperature. Then white intermediates of 2,3-dimethylbenzo[d]thiazol-3-ium 4-methylbenzenesulfonate powder was obtained by filtration and washed with a large amount of 1,2-dimethoxyethane solvent to remove remaining reagents. 2,3-dimethylbenzo[d]thiazol-3-ium 4-methylbenzenesulfonate (10.06 g, 30 mol) and 4-hydroxy-3,5-dimethylbenzaldehyde (4.51 g, 30 mol) were dissolved in methanol (250 mL) and then piperidine (1.18 ml, 12.0 mmol) was added in solution as catalyst. The solution was stirred at 50 °C for 48 h and then cooled to room temperature. After cooling the solution, dark red crystalline powder was obtained by filtration. The new compounds were purified by recrystallization process in methanol. The phase purity of HDB-T crystalline was confirmed by powder XRD (Fig. S2a). <sup>1</sup>H NMR (400 MHz, DMSO) δ 9.53 (s, 1H), 8.38 (d, J = 7.5 Hz, 1H), 8.19 (d, J = 8.4 Hz, 1H), 8.07 (d, J = 15.6 Hz, 1H), 7.88 - 7.68 (m, 5H), 7.47 (d, J = 8.1 Hz, 2H), 7.11 (d, J = 7.8 Hz, 2H), 4.30 (s, 3H), 2.27 (d, J = 15.0 Hz, 9H).

*Synthesis of 2-(4-hydroxystyryl)-3-methylbenzo[d]thiazol-3-ium 4-methylbenzenesulfonate (OHB-T):* 2,3-dimethylbenzo[d]thiazol-3-ium 4-methylbenzenesulfonate (10.06 g, 30 mmol) and 4-hydroxybenzaldehyde (3.66 g, 30

mmol) were dissolved in methanol (250 mL) and then piperidine (1.18 ml, 12.0 mmol) was added in solution as catalyst. The solution was stirred at 50 °C for 48 h and then cooled to room temperature. After cooling the solution, orange crystalline powder was obtained by filtration. The new compounds were purified by recrystallization process in methanol. The phase purity of OHB-T crystalline was confirmed by powder XRD (Fig. S2b). <sup>1</sup>H NMR (400 MHz, DMSO) δ 10.66 (s, 1H), 8.38 (d, *J* = 7.5 Hz, 1H), 8.18 (dd, *J* = 20.9, 12.1 Hz, 2H), 7.96 (d, *J* = 8.7 Hz, 2H), 7.88 - 7.69 (m, 3H), 7.47 (d, *J* = 8.1 Hz, 2H), 7.11 (d, *J* = 7.8 Hz, 2H), 6.94 (d, *J* = 8.7 Hz, 2H), 4.30 (s, 3H), 2.29 (s, 3H).

### Single-crystal X-ray structure analysis

The diffraction data were collected on a Rigaku AFC10 single-crystal diffractometer equipped with graphite-monochromated Cu K $\alpha$  radiation ( $\lambda$  = 1.54178 Å). The face-indexed absorption correction is carried out based on the XPREP program. Using Olex2,<sup>[1]</sup> the structures were solved using Intrinsic Phasing with the ShelXT<sup>[2]</sup> structure solution program and refined using Least Squares minimization with the ShelXL<sup>[3]</sup> refinement package. The ADDSYM algorithm from the program PLATON was used for structural verification,<sup>[4]</sup> and no higher symmetries were found. All of the hydrogen atoms were located on a difference Fourier map. The crystallographic data for the two new crystals is listed in Table S1.

### Single crystal growth

In order to obtain single crystals for initial optical tests, solubility of HDB-T was measured separately in methanol and mixed solution of methanol and acetonitrile

(1:1). As seen in Fig. S1a, mixed solvent system exhibited a higher solubility which indicates higher crystal growth rate. Then mixed solvent system was used to grow HDB-T crystals, and finally dark red bulk crystals with size around  $3 \times 2 \times 0.8 \text{ mm}^3$  and high optical quality was obtained, as seen in Fig. S1b.

### **Characterization**

The powder X-ray diffraction (XRD) patterns were recorded on Rigaku MiniFlex II diffractometer equipped with Cu K $\alpha$  radiation in the  $2\theta$  range of  $5-80^\circ$ .

Thermal gravimetric analysis (TGA) was performed on a NETZSCH STA 449F5 TG/DTA instruments, and a heating rate of  $10^\circ\text{C min}^{-1}$  in nitrogen was adopted.

The diffuse reflectance data were collected with a UH4150 UV-visible spectrophotometer with a diffuse reflectance accessory in the range of 250 nm to 1500 nm. The absorption spectra were calculated from the reflectance spectra using the Kubelka-Munk function:  $\alpha/S = (1-R)^2/2R$ , where  $\alpha$  is the absorption coefficient,  $S$  is the scattering coefficient, and  $R$  is the reflectance, respectively.<sup>[5]</sup> The UV-vis spectra of in methanol solution ( $1 \times 10^{-5} \text{ mol}\cdot\text{L}^{-1}$ ) were measured via a UH4150 UV-visible spectrophotometer.

The infrared spectrum was recorded in the region of  $400-2000 \text{ cm}^{-1}$  using an infrared spectrometer model Excalibur 3100 using a KBr tablet method.

Raman spectroscopy was measured using a Via-Reflex Raman spectrometer manufactured by Renishaw, Inc., with an excitation wavelength of 785 nm and a scanning range of  $50-3600 \text{ cm}^{-1}$ .

Optical SHG tests of HDB-T and OHB-T were performed on the powder

samples by means of the Kurtz–Perry method.<sup>[6]</sup> Fundamental 2.09  $\mu\text{m}$  light was generated with a Q-switched Ho:Tm:Cr:YAG laser. Different particle sizes powders were prepared separately by mechanical grinding of the single crystals.

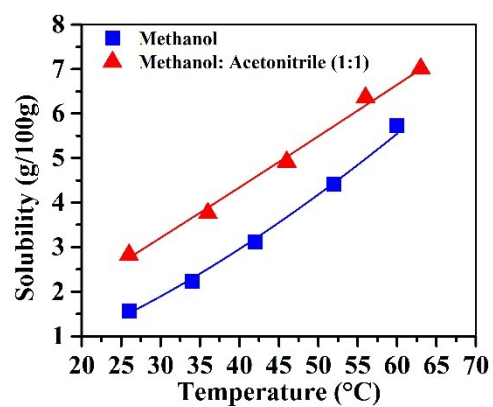
### **Computational methods**

The density functional theory calculations based on plane-wave pseudopotential method for HDB-T and OHB-T crystals were performed by CASTEP package.<sup>[7]</sup> The optimized norm-conserving pseudopotentials<sup>[8]</sup> were utilized to model the ion-electron interaction for all constituent elements. The kinetic energy cutoffs of 950 eV and Monkhorst-Pack k-point meshes<sup>[9]</sup> with the spanning of less than  $0.05/\text{\AA}^3$  ( $2\times 4\times 1$  for HDB-T and  $3\times 2\times 1$  for OHB-T in the first Brillouin zone were chosen. The generalized gradient approximation with solid Perdew–Burke–Ernzerhof (PBEsol) exchange-correlation functional<sup>[10]</sup> was adopted. The lattice constants were fixed and all atom positions were fully optimized in DFT calculations. The linear response method<sup>[11]</sup> was employed to calculate the phonon dispersion, infrared and Raman spectrum ( $\lambda = 532 \text{ nm}$ ,  $T=300 \text{ K}$ ) with smearing wavenumber of  $2 \text{ cm}^{-1}$ . Our tests revealed that the above computational parameters were sufficiently accurate for present purposes.<sup>[12-14]</sup> The specific IR and Raman vibrational modes were assigned by Vibrational Analysis module in CASTEP package.

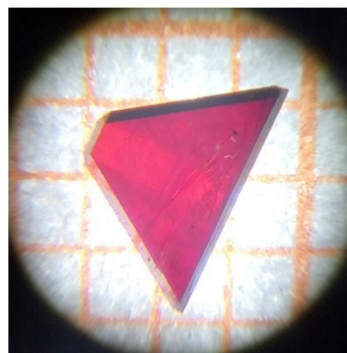
### **Terahertz-wave generation**

The schematic diagram of DFG system with HDB-T crystal is illustrated in Fig. 4a. A double-pass optical parametric oscillator, consisting of cavity mirrors (M2&M3), KTP1 and KTP2 crystals ( $7\times 10\times 15 \text{ mm}^3$ ,  $\theta=65^\circ$ ,  $\phi=0^\circ$ ) rotated by

galvano-optical beam scanners (Cambridge Technology, 6230H), was pumped by the 532 nm green light, generated by second harmonic generation (SHG) in KTP ( $7 \times 7 \times 10$  mm<sup>3</sup>,  $\theta=90^\circ$ ,  $\varphi=23.5^\circ$ ) crystal. M1 and dichroic mirror (DM) were utilized to reflect and block the 532 nm pump wave, respectively. One of the tunable dual-wavelength pump  $\lambda_2$  was tuned in the range of 1.36 - 1.5  $\mu\text{m}$  by rotating KTP2 and the other was fixed ( $\lambda_1 = 1.364 \mu\text{m}$ ). The HDB-T crystal was pumped with the dual-wavelength pump wave focused by a convex lens (M4,  $f=200$  mm) in order to achieve the high intensity.



(a)



(b)

**Fig. S1.** (a) The solubility of HDB-T in methanol; (b) photograph of HDB-T single crystal grown from methanol and acetonitrile (1:1).

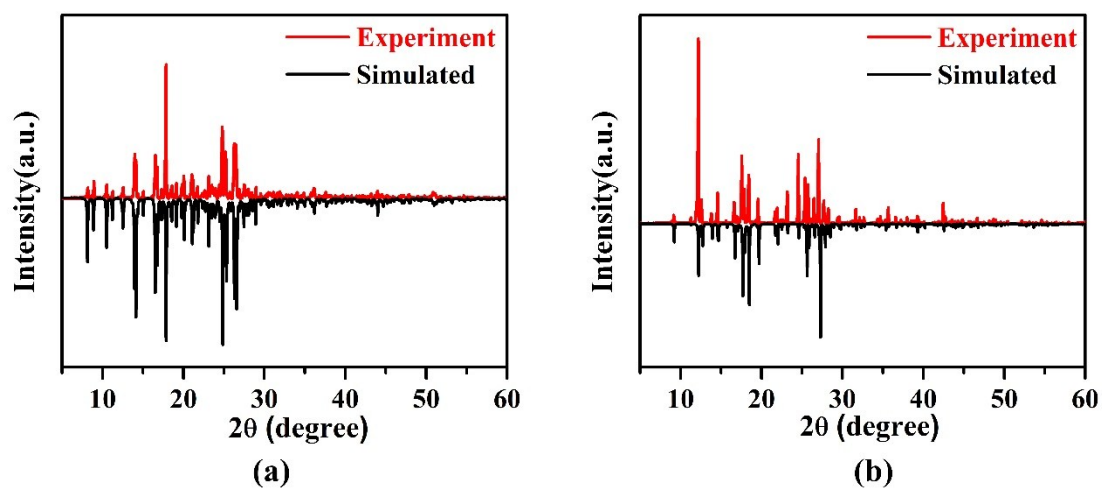


**Fig. S2.** Experimental and simulated X-ray powder diffraction patterns of (a) HDB-T and (b) OHB-T.



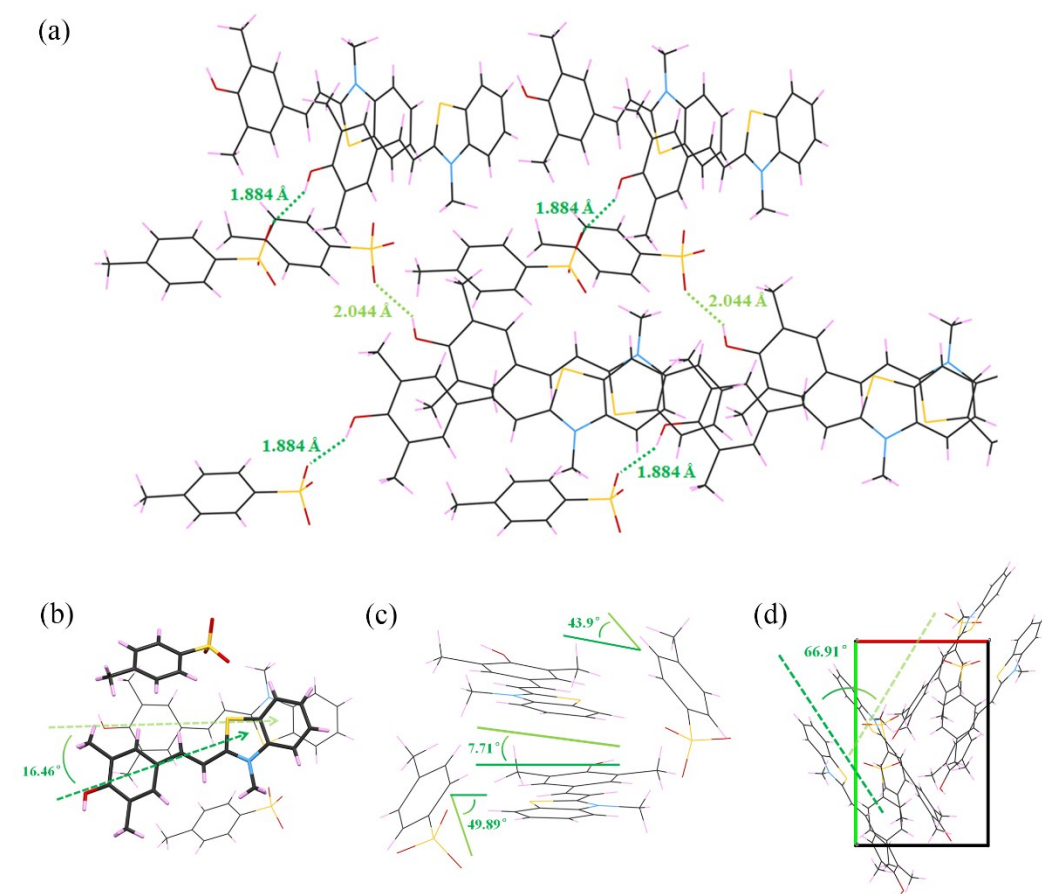


**Fig. S3.** (a) two kinds of hydrogen bonds in the crystal structure of HDB-T. (b) packing form of two cation in one layer. (c) the angle between two cations in one layer and the angle between cations and anions. (d) the angles between neighboring cation layers.

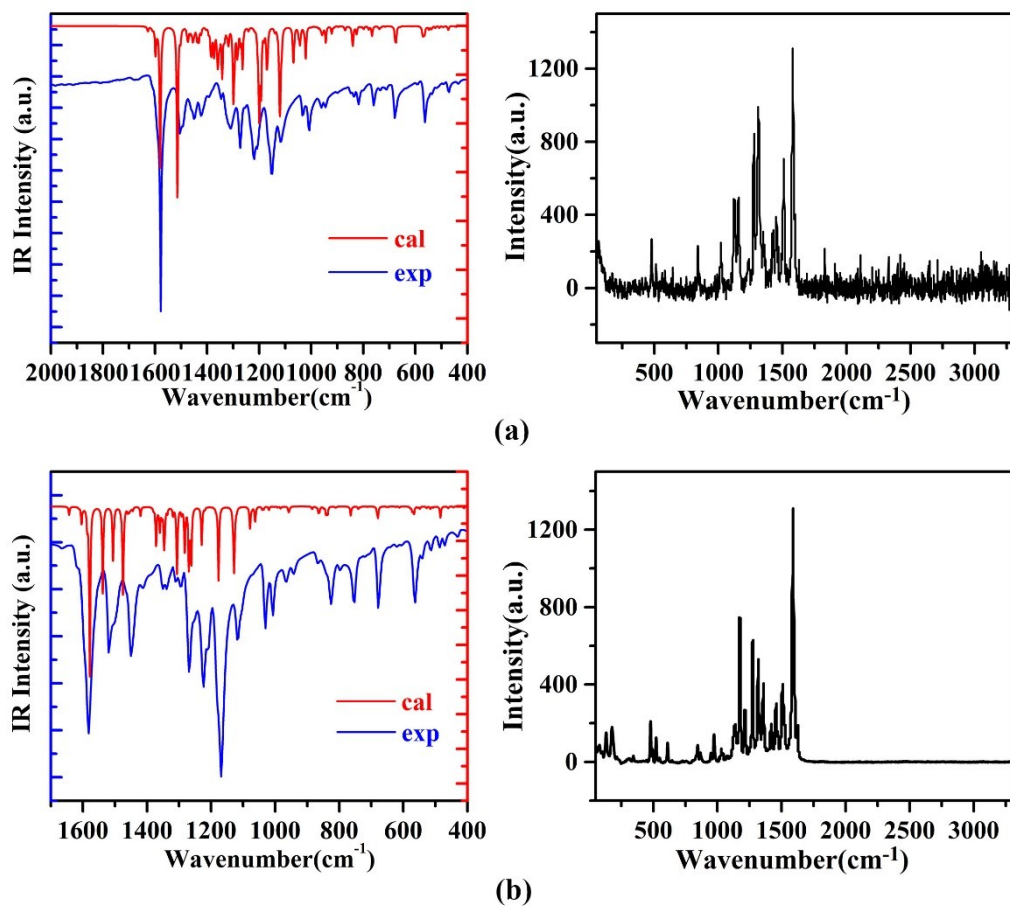


**Fig. S4.** IR and Raman spectra of (a) HDB-T and (b) OHB-T.

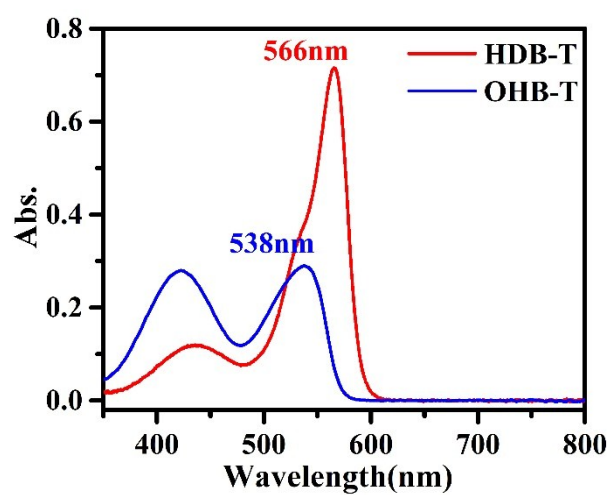


**Fig. S5.** UV-vis absorption spectra in methanol solution ( $1 \times 10^{-5}$  M) of HDB-T and OHB-T crystals.

**Table S1.** Crystal data and structure refinement for HDB-T and OHB-T <sup>a</sup>

	<b>HDB-T</b>	<b>OHB-T</b>
Formula	C <sub>25</sub> H <sub>25</sub> NO <sub>4</sub> S <sub>2</sub>	C <sub>23</sub> H <sub>21</sub> NO <sub>4</sub> S <sub>2</sub>
Fw	467.60	439.53
Crystal system	Monoclinic	Orthorhombic
Space group	<i>P</i> 2 <sub>1</sub>	<i>P</i> ca2 <sub>1</sub>
<i>a</i> (Å)	8.5863(10)	15.6034(10)
<i>b</i> (Å)	12.9740(10)	6.9414(10)
<i>c</i> (Å)	20.2400(2)	19.1717(2)
<i>α</i> (deg)	90	90
<i>β</i> (deg)	101.1440(10)	90
<i>γ</i> (deg)	90	90
V (Å <sup>3</sup> )	2212.19(4)	2076.48(4)
Z	4	4
GOF on F <sup>2</sup>	1.074	1.075
R <sub>1</sub> (>2σ( <i>I</i> ))	0.0340	0.0351
wR <sub>2</sub> (all data)	0.0852	0.0970
CCDC No	1901961	1901962

<sup>a</sup>  $R(F) = \sum ||F_o| - |F_c|| / \sum |F_o|$  for  $F_o > 2\sigma(F_o)$ .  $R_w(F_o) = \{\sum [w(F_o - F_c)^2] / \sum w F_o^4\}^{1/2}$  for all data.

## Note and references

- [1] O. V. Dolomanov, L. J. Bourhis, R. J. Gildea, J. A. K. Howard, H. Puschmann, *J. Appl. Crystallogr.* **2009**, 42, 339-341.
- [2] G. M. Sheldrick, *Acta Crystallogr., Sect. A: Found. Adv.* **2015**, 71, 3-8.
- [3] G. M. Sheldrick, *Acta Crystallogr., Sect. C: Struct. Chem.* **2015**, 71, 3-8.
- [4] A. L. Spek, *J. Appl. Crystallogr.* **2003**, 36, 7-13.
- [5] a) P. Kubelka, F. Munk, *Z. Tech. Phys* **1931**, 12, 593; b) J. Tauc, *Mater. Res. Bull.* **1970**, 5, 721-729.
- [6] S. K. Kurtz and T. T. Perry, *J. Appl. Phys.* **1968**, 39, 3798-3813.
- [7] S. J. Clark, M. D. Segall, C. J. Pickard, P. J. Hasnip, M. J. Probert, K. Refson, M. C. Payne, *Z. Kristallogr.* **2005**, 220, 567-570.
- [8] A. M. Rappe, K. M. Rabe, E. Kaxiras, J. D. Joannopoulos, *Phys. Rev. B* **1990**, 41, 1227-1230.
- [9] H. J. Monkhorst, J. D. Pack, *Phys. Rev. B* **1976**, 13, 5188-5192.
- [10] J. P. Perdew, K. Burke, M. Ernzerhof, *Phys. Rev. Lett.* **1996**, 77, 3865-3868.
- [11] S. Baroni, S. de Gironcoli, A. Dal Corso, P. Giannozzi, *Rev. Mod. Phys.* **2001**, 73, 515-562.
- [12] A. P. Yelisseyev, L. I. Isaenko, P. Krinitsin, F. Liang, A. A. Goloshumova, D. Y. Naumov, Z. S. Lin, *Inorg. Chem.* **2016**, 55, 8672-8680.
- [13] T. Sun, F. Liang, X. Zhang, H. Tu, Z. Lin, G. Zhang, Y. Wu, *Polyhedron* **2017**, 127, 478-488.
- [14] A. Yelisseyev, F. Liang, L. Isaenko, S. Lobanov, A. Goloshumova, Z. S. Lin, *Opt. Mater.* **2017**, 72, 795-804.